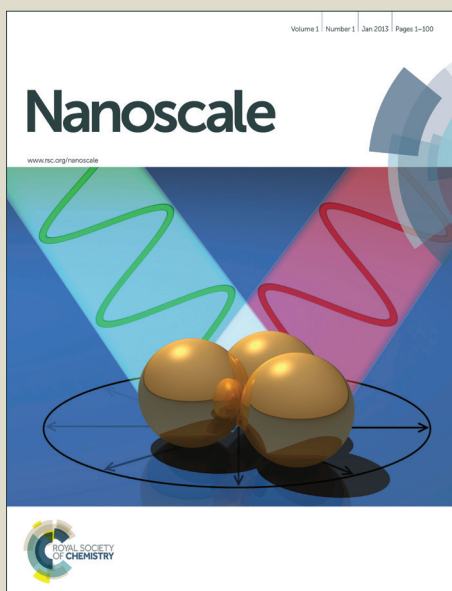


Nanoscale

Accepted Manuscript



This is an *Accepted Manuscript*, which has been through the Royal Society of Chemistry peer review process and has been accepted for publication.

Accepted Manuscripts are published online shortly after acceptance, before technical editing, formatting and proof reading. Using this free service, authors can make their results available to the community, in citable form, before we publish the edited article. We will replace this *Accepted Manuscript* with the edited and formatted *Advance Article* as soon as it is available.

You can find more information about *Accepted Manuscripts* in the [Information for Authors](#).

Please note that technical editing may introduce minor changes to the text and/or graphics, which may alter content. The journal's standard [Terms & Conditions](#) and the [Ethical guidelines](#) still apply. In no event shall the Royal Society of Chemistry be held responsible for any errors or omissions in this *Accepted Manuscript* or any consequences arising from the use of any information it contains.

Cite this: DOI: 10.1039/c0xx00000x

www.rsc.org/xxxxxx

ARTICLE TYPE

Packaged triboelectric nanogenerator with high durability for severe environment

Long Gu^a, Nuanyang Cui^a, Jinmei Liu^a, Youbin Zheng^a, Suo Bai^{a,b} and Yong Qin^{a,b,*}*Received (in XXX, XXX) Xth XXXXXXXXX 20XX, Accepted Xth XXXXXXXXX 20XX*

DOI: 10.1039/b000000x

Many factors in the environment (such as dust, moisture and rain) severely influence the output performance of triboelectric nanogenerator (TNG), which greatly limits its application. In this work, we designed and fabricated a kind of packaged TNG (PTNG) that can work normally in dust and humidity for harvesting the noise energy. Under a sound wave of 110 dB and 200 Hz, the PTNG can generate a maximum output voltage of 72 V and a maximum output current of 0.66 mA. In the structure of PTNG, the frictional layer is fully isolated from ambient environment, which makes it work steadily in dusty and humid conditions without any damping of output performance. Moreover, it can be used as a stable power source to directly light up 24 red commercial light emitting diodes (LEDs) driven by sound even in the severely raining environment. This PTNG has a great potential to be applied in real environment, which is critically important to the application of TNG.

Introduction

In the past decades, more and more efforts have been devoted to harvesting mechanical energy from ambient environment to get sustainable power supply for the tremendous micro/nano devices¹⁻⁸. As a common form of mechanical energy, sound energy exists anywhere and anytime in our environment, but is often wasted owing to lacking of effective harvesting methods^{9,10}. Although sound energy has been scavenged by approaches based on piezoelectric effect¹¹⁻¹³ and electrostatic effect¹⁴ in previous works, their application is limited by low energy conversion efficiency^{11,12}, complex structure¹³ and high requirement for materials¹⁴. Recently, the newly invented triboelectric nanogenerator has been proved to be a simple, low-cost and effective technology to harvest various forms of mechanical energy and convert them into electric energy¹⁵⁻²⁴. The energy conversion is achieved by coupling between triboelectrification and electrostatic induction. When two materials with different triboelectric polarity contact and rub with each other, surface charge will transfer from one material to the other. Then periodic contact and separation of the oppositely charged surfaces can generate an induced potential difference between two electrodes, which drives the alternating flow of electrons through an external circuit. Lately, several works have been reported to harvest sound energy based on this technology²⁵⁻²⁷. Compared with the

previously reported sound harvesters, the sound driven triboelectric nanogenerator (STNG) greatly improved the sound energy conversion efficiency and the output performance. But these STNGs have an open structure, which is commonly used in most reported TNGs. As the whole internal structure is exposed to the environment, these TNGs can't work normally in severe environment such as in dust and moisture environment. Dust can easily adsorb to the frictional surfaces of TNG, then hinder the contact of frictional surfaces, resulting in the decrease of TNG's output. In addition, the moisture adsorbed on frictional surface can also increase the conductivity of friction layer, and then discharging occurs on the surfaces, leading to the decrease of TNG's output²⁸. Thus, these factors in the environment could greatly influence the state of the frictional surface and reduce the output performance of the TNG. But for a sound harvester, it needs to work under different environments, such as a very humid place or a dusty region, or a rainy district. These diverse application conditions require the STNG to have high durability and the ability of working normally in these severe working conditions. Therefore, a sound harvester which has not only excellent output performance but also outstanding environmental stability in severe working condition is urgently needed.

In this work, we developed a high robust sound driven PTNG by integrating polyethylene (PE) film and multihole polyvinyl

chloride (PVC) plate. Its maximum output voltage and current can reach 72 V and 0.66 mA, respectively. By isolating the frictional surface of PTNG from ambient environment, it could work steadily in dusty and humid conditions. Moreover, it can stably and directly light up 24 red commercial LEDs without energy storage process even in the severe raining condition.

Results and Discussion

As schematically illustrated in Figure 1a, the PTNG consists of four parts: a multihole PVC plate covered with a layer of Al (Al@PVC), a PE film with Ag electrode on one side and polyvinylidene fluoride (PVDF) nanofibers (scanning electron microscope image shown in Figure 1b) on the other side (Part A), a PE film with Ag electrode on one side (Part B) and two spacers. These components are connected using double-side tape along their four edges to construct the drum-like PTNG. In the sealed structure, the multihole PVC plate acts as the skeleton of the PTNG, and the Al coated on it plays dual roles of a frictional surface and an electrode. A large number of through-holes on the PVC plate could greatly reduce the attenuation of sound when it propagates through the plate. The internal surfaces of Part A and Part B act as the frictional layers in the PTNG and hierarchically convert the sound energy, which improves the utilization efficiency. Moreover, Part A and Part B can fully isolate the frictional layer of the PTNG from ambient environment realizing effective protection for the device from negative influences. Two spacers connect Part A and Part B with PVC plate, creating a cavity at the center between them for the vibration of Part A and Part B. Figure 1c shows a full cycle of electricity generation process of the PTNG. In the figure, Al@PVC is replaced by a layer of Al to simplify the diagram. At the initial state, Part A and Part B are not in contact with Al layer, and there is no charge existing on them (Figure 1c I). When the device is driven by a sound wave, Part A and Part B will vibrate at the same frequency of the sound wave. Once the internal surface of Part A or Part B contacts and rubs with the Al layer, charges will transfer between them. According to the triboelectric series, electrons are injected from Al to PVDF in Part A and PE in Part B, generating negative charges on PVDF and PE (Figure 1c II). When the PVDF in Part A is fully contacted with Al layer (Figure 1c III), the Ag electrode on Part A possesses a higher electric potential than Al electrode. As a result, the free charges flow from Al electrode to Ag electrode through the external circuit to balance the potential difference. Subsequently, the Al layer will reach the middle of

Part A and Part B. Meanwhile, the electric potential of Ag electrode in Part A is dropped and lower than that of Al electrode, so the charges flow back in the opposite direction from Ag electrode to Al electrode (Figure 1c IV). As the vibration continues, the Al layer then contacts with Part B (Figure 1c V). In this state, triboelectric charges on PE induce a higher electric

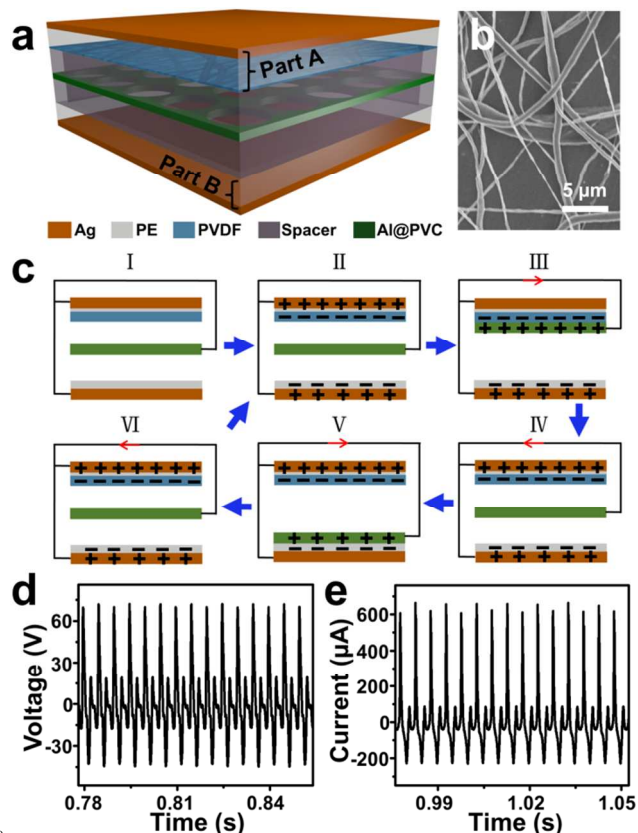


Fig. 1 (a) Structure illustration of the PTNG. (b) Scanning electron microscope image of PVDF nanofibers. (c) Sketches of the electricity generation process in a full cycle. The red arrows indicate the direction of current. (d, e) The open-circuit voltage and short-circuit current of the PTNG.

potential on Ag electrode in Part B than Al electrode, which drives the free charges to flow from Al electrode to Ag electrode to screen the potential difference. When the vibration reverts back to the state II, the distribution of charges returns to the state II as well (Figure 1c VI), and a cycle of electricity generation process is fully completed. In summary, when Part A and Part B vibrate up and down, the PTNG acts as an electron pump that drives electrons to flow back and forth between the Ag and Al electrodes, producing an alternating current with four pulses in each period. Figure 1d and e show the output voltage and current of the PTNG. Driven by the sound wave of 110 dB and 200 Hz, the PTNG generates an output voltage of 72 V and an output current of 0.66 mA. The period of the output signals is 5 ms, and two positive and two negative peaks can be observed in each

cycle, which corresponds well with the PTNG's working process discussed above.

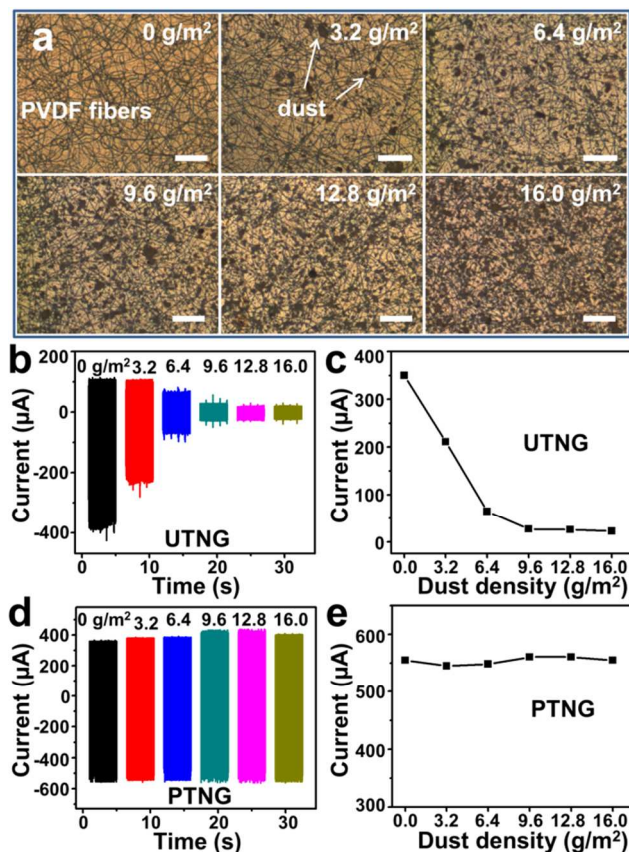


Fig. 2 (a) Optical images of PVDF nanofibers on PE film covered by 0, 3.2, 6.4, 9.6, 12.8, 16.0 g/m² dust, respectively. All scale bars are 100 μm. (b, d) The output current of UTNG and PTNG under different dust density. (c, e) The relationship between current peak values and dust density.

In order to investigate the influence of environmental factors on STNG, dusty, humid and rainy conditions were used as the working environment to test the output performance of STNG. As a comparison, an unsealed TNG (UTNG) was also fabricated as a control group, which just contains one PE film with PVDF nanofibers, a multihole PVC substrate and a spacer. Compared with the PTNG, the PE film without PVDF nanofibers is removed in its structure. Thus, the internal structure of the UTNG is completely exposed to the environment. First of all, the impact of dust on the output performance of UTNG and PTNG was investigated to examine the anti-dust capability of the PTNG. In this experiment, the two kinds of STNGs were both put into an enclosed box (25 cm × 25 cm × 18 cm) and then 0.2 g dust was blew into the space to guarantee the dust deposited on these two STNGs with same density. By repeating the above operation, we could deposit different amounts of dust on the two devices. For the UTNG, the dust particles could easily diffuse into its internal structure along with air, and then adsorb on its frictional surfaces.

Figure 2a shows the optical images of the PVDF nanofibers covered by 0, 3.2, 6.4, 9.6, 12.8, 16.0 g/m² dust, respectively. It can be easily seen that more and more PVDF nanofibers are covered by dust particles with the increase of dust density. These dust particles will severely hinder the contact of PVDF with Al, leading to a sharp decrease of the UTNG's output current (Figure 2b). In this process, a sound wave of 103 dB and 200 Hz was used to driven the two STNGs. The statistic result in Figure 2c shows that the current peak value of the UTNG decreases from 390 μA to 24.5 μA (dropped by 93.7%) after 16 g/m² dust deposited on the device. While for the PTNG, the whole device is sealed and the dust cannot reach the internal frictional materials. Thus, its output current changes little with the increase of dust density (Figure 2d). The statistic result in Figure 2e reveals that the current peak value of the PTNG keeps stable at about 560 μA all the time, which indicates that the PTNG is very dustproof and could work steadily in dusty environment.

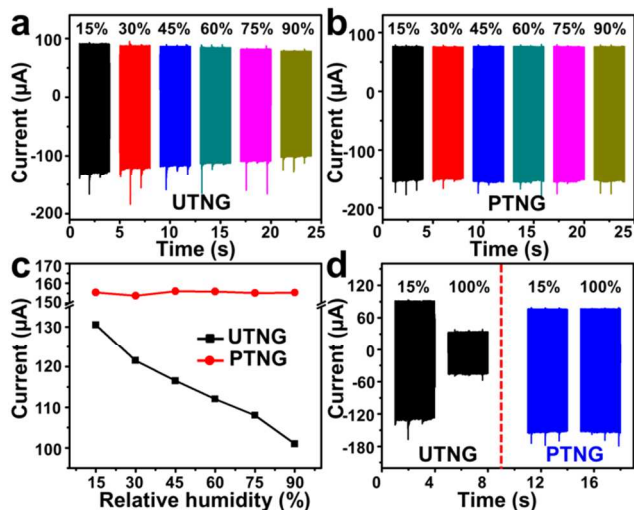


Fig. 3 (a, b) The output current of UTNG and PTNG under different RH. (c) The relationship between current peak values and RH. (d) The output current of UTNG and PTNG at RH of 15% comparing with their output current after keeping at RH of 100% for 5 h. Percentages inset in (a), (b) and (d) are the RH at room temperature.

Besides the dust, moisture can influence the output performance of TNG through changing the conductivity of frictional layer. In order to examine the anti-humidity capability of PTNG, the influences of humidity on the output performance of UTNG and PTNG were investigated. In this part, the two devices were placed into the enclosed box with controlled relative humidity (RH), and driven by a sound wave of 90 dB and 200 Hz. Figure 3a and b show the output current of the UTNG and PTNG with RH ranging from 15% to 90% in steps of 15% at room temperature. The output current of the UTNG decreases

with the increase of RH, while the output current of the PTNG displays no change. With the RH increases from 15% to 90%, the current peak value of UTNG decreases from 130 μA to 101 μA (dropped by 22.3%), while the current peak value of the PTNG keeps at about 156 μA without obviously change as shown in Figure 3c. Furthermore, the RH in the box was increased to 100%, and then these two STNGs were kept in this condition for 5 hours. The corresponding output current of the UTNG decreases to about 45 μA (dropped by 65.4% compared with that under the RH of 15%), as shown in Figure 3d. While the output current of the PTNG still remains at about 156 μA (Figure 3d). These results indicate that the PTNG has an excellent performance on resisting moisture and could work steadily in humid environment.

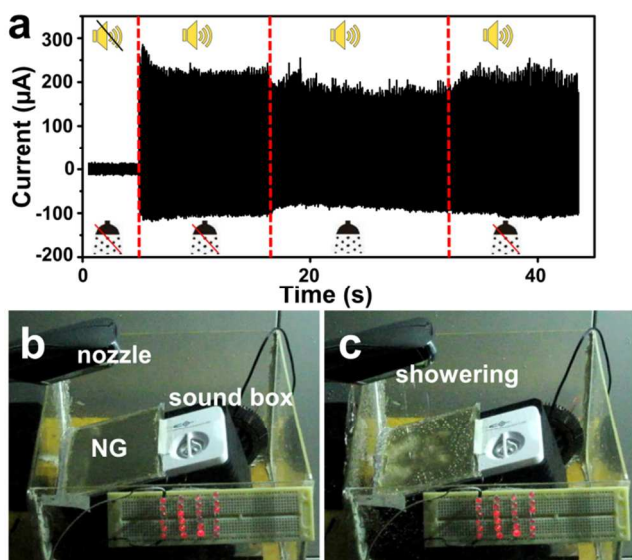


Fig. 4 (a) The output current of the PTNG under a rainy condition simulated by shower nozzle. (b, c) 24 red commercial LEDs lighted up by the PTNG with the shower nozzle off (b) and on (c).

Except the dust and moisture, STNG is still inevitable to face some extreme conditions when it works outdoors, such as rain. A large amount of rainwater can promote the environmental RH to 100% and infiltrate into the internal structure of TNG, which will greatly reduce the output performance of the TNG²⁹. Here, a rainy condition was simulated by using a shower nozzle, and the output performance of the PTNG was measured in this case. As shown in Figure 4a and Video S1, the output current of the PTNG is about 230 μA before opening the shower nozzle. Once the nozzle is open, the water drops fall on the surface of the PTNG. Meanwhile, the output current of the PTNG decreases to about 180 μA . When closing the nozzle, the output current gradually returns to about 230 μA . The decrease and recovery of the output current in this process is attributed to the following reason. When

the shower nozzle is on, water drops fall on the surface of PTNG and the weight on PE film increases. Thus, the amplitude of PE films decrease simultaneously, resulting in a small decrease of the PTNG's output. When the shower nozzle is closed, the water on the device will be flicked off by the vibrating PE films. Then the device returns to its original state and the output current reverts back as well. Although the output current of PTNG is slightly decreased under the showering, it is still enough to power many electronic devices. Here, the PTNG was used to power 24 red commercial LEDs (Figure 4b). Obviously, the brightness of these LEDs changes little before and after water drops falling on the PTNG as shown in Figure 4c and Video S2, which demonstrates that the PTNG could work normally in rainy circumstance to be a stable power supply.

Conclusions

In summary, we developed a PTNG and investigated the influence of dust and moisture on its output performance. The maximum output voltage and current of the PTNG are up to 72 V and 0.66 mA, respectively. It works steadily in dusty and humid environment. Moreover, it can be used to stably light up 24 red commercial LEDs even in the simulated rain. This kind of PTNG has great potential to be applied in severe environment such as in dusty, humid and rainy conditions, which paves the way for the practical application of triboelectric nanogenerator.

Experimental Section

Fabrication of the PTNG

Firstly, a thin layer of Al is deposited on both sides of the multihole PVC plate (10 cm \times 10 cm \times 0.5 mm) by magnetron sputtering to get the Al coated PVC plate. Secondly, A piece of PE film (thickness of 5 μm) is covered by PVDF nanofibers on one side by electrospinning and deposited with Ag on the other side by magnetron sputtering, which is marked as Part A. And another piece of PE film is only deposited with Ag on one side by magnetron sputtering, which is marked as Part B. Thirdly, two spacers (thickness of 30 μm) are glued along the edges of the PVC plate on both sides. After that, Part A is glued on one spacer and Part B is glued on the other spacer with Ag electrodes outside, as shown in Figure 1a. Here, Layer A and Layer B have two roles. On one hand, both of their inner surfaces are used as the frictional surface to work with Al on PVC plate. On the other hand, they are used as the packing materials to pack the top and

the bottom of the device, respectively. Finally, the fabricated device is sealed along the edges with sealant, which cooperates with the packing top of Layer A and the packing bottom of Layer B to realize a fully packaged structure. At the same time, the Ag deposited on Part A and Part B are connected together as one electrode and the Al deposited on PVC plate acts as the other electrode for the subsequently electric measurement.

Electrospinning of the PVDF nanofiber

3.75 g PVDF, 8.5 g N,N-dimethylacetamide (DMAC) and 12.75 g acetone are mixed in a triangular flask and stirred at 60 °C for 30 min to form a uniformly solution. Then the solution is added into a syringe. Electrospinning is conducted at 15 kV with the feed rate of 3 mL/h, and the distance between needle and collector is 16 cm.

Controlling of RH

A humidifier, a mini fanner and a thermohygrometer are installed into an inclosed box before measurement. Humidifier is used to adjust the content of moisture, and the fanner is used to speed the uniformly distributing of moisture in the space. The thermohygrometer is used to monitor the RH and temperature in the space. Through real-time monitoring and meticulous adjusting, the desired RH can be achieved.

Acknowledgements

Research was supported by NSFC (NO. 51322203, 51472111), the National Program for Support of Top-notch Young Professionals, the Fundamental Research Funds for the Central Universities (No. lzujbky-2014-m02, lzujbky-2015-118, lzujbky-2015-208), PCSIRT (NO. IRT1251).

Notes and references

^a Institute of Nanoscience and Nanotechnology, School of Physical Science and Technology, Lanzhou University, Lanzhou, 730000, China.

* To whom correspondence should be addressed, E-mail: qinyong@lzu.edu.cn

^b The Research Institute of Biomedical Nanotechnology, Lanzhou University, Lanzhou 730000, China

† Electronic Supplementary Information (ESI) available. See DOI:10.1039/b000000x/

- J. A. Paradiso, T. Starner, *IEEE Perva. Comput.*, 2005, **4**, 18-27.
- E. Bouendeu, A. Greiner, P. J. Smith, J. G. Korvink, *IEEE Sens. J.*, 2011, **11**, 107-113.
- S. P. Beeby, M. J. Tudor, N. M. White, *Meas. Sci. Technol.*, 2006, **17**, 175-195.
- M. S. Dresslhaus, I. L. Tomas, *Nature*, 2001, **414**, 332-337.
- Z. L. Wang, J. H. Song, *Science*, 2006, **312**, 242-246.
- Y. Qin, X. D. Wang, Z. L. Wang, *Nature*, 2008, **451**, 809-813.
- Y. F. Hu, L. Lin, Y. Zhang, Z. L. Wang, *Adv. Mater.*, 2011, **10**, 5025-5031.

- K. I. Park, J. H. Son, G. T. Hwang, C. K. Jeong, J. Ryu, M. Koo, I. Choi, S. H. Lee, M. Byun, Z. L. Wang, K. J. Lee, *Adv. Mater.*, 2014, **26**, 2514-2520.
- S. B. Horowitz, M. Sheplak, L. N. Cattafesta III, T. Nishida, *J. Micromech. Microeng.*, 2006, **16**, 174-181.
- X. D. Wang, J. H. Song, J. Liu, Z. L. Wang, *Science*, 2007, **316**, 102-105.
- C. Xu, X. D. Wang, Z. L. Wang, *J. Am. Chem. Soc.*, 2009, **131**, 5866-5872.
- S. N. Cha, J. S. Seo, S. M. Kim, H. J. Kim, Y. J. Park, S. W. Kim, J. M. Kim, *Adv. Mater.*, 2010, **22**, 4726-4730.
- B. Li, J. H. You, Y. J. Kim, *Smart Mater. Struct.*, 2013, **22**, 055013.
- R. Que, Q. Shao, Q. L. Li, M. Shao, S. D. Cai, S. D. Wang, S. T. Lee, *Angew. Chem.*, 2012, **124**, 5514-5518.
- N. Y. Cui, J. M. Liu, L. Gu, S. Bai, X. B. Chen, Y. Qin, *ACS Appl. Mater. Interfaces*, 2015, **7**, 18225-18230.
- Y. B. Zheng, L. Cheng, M. M. Yuan, Z. Wang, L. Zhang, Y. Qin, T. Jing, *Nanoscale*, 2014, **6**, 7842.
- F. R. Fan, L. Lin, G. Zhu, W. Z. Wu, R. Zhang, Z. L. Wang, *Nano Lett.*, 2012, **12**, 3109-3114.
- G. Zhu, J. Chen, Y. Liu, P. Bai, Y. S. Zhou, Q. S. Jing, C. F. Pan, Z. L. Wang, *Nano Lett.*, 2013, **13**, 2282-2289.
- L. Zhang, L. Cheng, S. Bai, C. Su, X. B. Chen, Y. Qin, *Nanoscale*, 2015, **7**, 1285-1289
- J. W. Zhong, Y. Zhang, Q. Z. Zhong, Q. Y. Hu, B. Hu, Z. L. Wang, J. Zhou, *ACS Nano*, 2014, **8**, 6273-6280.
- Z. Wang, L. Cheng, Y. B. Zheng, Y. Qin, Z. L. Wang, *Nano Energy*, 2014, **10**, 37-43.
- J. Yang, J. Chen, Y. Liu, W. Q. Yang, Y. J. Su, Z. L. Wang, *ACS Nano*, 2014, **8**, 2649-2657.
- N. Y. Cui, L. Gu, J. M. Liu, S. Bai, J. W. Qiu, J. C. Fu, X. L. Kou, H. Liu, Y. Qin, Z. L. Wang, *Nano Energy*, 2015, **15**, 321-328.
- J. M. Liu, N. Y. Cui, L. Gu, X. B. Chen, S. Bai, Y. B. Zheng, C. X. Hu, Y. Qin, *Nano Energy*, submitted.
- K. Y. Lee, J. Chun, J. H. Lee, K. N. Kim, N. R. Kang, J. Y. Kim, M. H. Kim, K. S. Shin, M. K. Gupta, J. M. Baik, S. W. Kim, *Adv. Mater.*, 2014, **26**, 5037-5042.
- A. F. Yu, M. Song, Y. Zhang, L. B. Chen, J. Y. Zhai, Z. L. Wang, *Nano Res.*, 2015, **8**, 765-773.
- K. N. Kim, J. Chun, J. W. Kim, K. Y. Lee, J. U. Park, S. W. Kim, Z. L. Wang, J. M. Baik, *ACS Nano*, 2015, **9**, 6394-6400.
- V. Nguyen, R. S. Yang, *Nano Energy*, 2013, **2**, 604-608.
- Y. Yang, H. L. Zhang, R. Y. Liu, X. N. Wen, T. C. Hou, Z. L. Wang, *Adv. Energy Mater.*, 2013, **3**, 1563-1568.